ACS Photonics

Article

pubs.acs.org/journal/apchd5

Antenna–Cavity Hybrids: Matching Polar Opposites for Purcell Enhancements at Any Linewidth

Hugo M. Doeleman,*[,†,‡] Ewold Verhagen,[†] and A. Femius Koenderink*[,†,‡]

[†]Center for Nanophotonics, FOM Institute AMOLF, Science Park 104, 1098 XG Amsterdam, The Netherlands

[‡]van der Waals-Zeeman Institute, University of Amsterdam, Science Park 904, P.O. Box 94485, 1090 GL Amsterdam, The Netherlands

Supporting Information

ABSTRACT: Strong interaction between light and a single quantum emitter is essential to a great number of applications, including single photon sources. Microcavities and plasmonic antennas have been used frequently to enhance these interactions through the Purcell effect. Both can provide large emission enhancements: the cavity typically through long photon lifetimes (high Q), and the antenna mostly through strong field enhancement (low mode volume V). In this work, we demonstrate that a hybrid system, which combines a cavity and a dipolar antenna, can achieve stronger emission enhancements than the cavity or antenna alone. We show that these systems can in fact break the fundamental limit on single antenna enhancement. Additionally, hybrid systems can be used as a versatile platform to tune the bandwidth of enhancement to any desired value between that of the cavity and the antenna, while simultaneously boosting emission enhancement. Our fully self-consistent analytical model allows to identify the underlying mechanisms of boosted emission enhancement in hybrid systems, which include radiation damping and constructive interference between multiple-scattering paths. Moreover, we find excellent agreement between strongly boosted enhancement spectra from our analytical model and from finite-element simulations on a realistic cavity–antenna system. Finally, we demonstrate that hybrid systems can simultaneously boost emission enhancement and maintain a near-unity outcoupling efficiency into a single cavity decay channel, such as a waveguide.

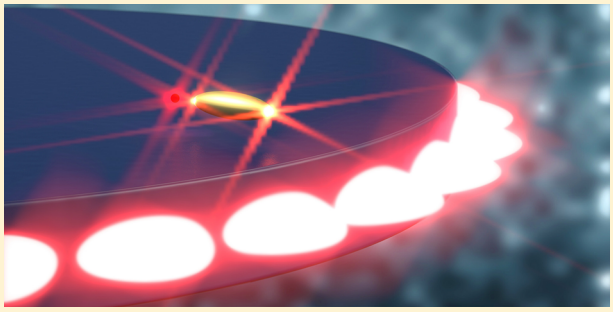

KEYWORDS: *hybrid systems, microcavities, plasmonic antennas, Purcell enhancement, single-photon sources, quantum optics*

For many nanophotonic applications, such as single photon sources operated at high frequency,[1−3] nanoscale lasers,[4] quantum logical gates for photons,[5,6] and highly sensitive, low detection volume sensing devices,[7−9] strong interactions between a single quantum emitter and light are vital. This interaction can be enhanced by coupling emitters to nanophotonic structures that enhance their emission rates using the Purcell effect.[10] Tradionally, this is done by placing emitters in dielectric microcavities. The relative emission enhancement of an emitter at resonance with a cavity mode, that is, the Purcell factor (F_P), then relates to the quality factor (Q) and the mode volume (V) as

$$F_P = (3/(4\pi^2))(\lambda/n)^3(Q/V) \quad (1)$$

with n the index of the medium around the emitter. Microcavity modes typically reach large enhancements because of their long photon lifetimes and consequently high quality factors.[11] Additionally, most light is then emitted into a single cavity mode, facilitating efficient collection through, for example, a waveguide, which is a major advantage for applications such as single photon sources.[3,12] Plasmonic nanoantennas are a popular alternative solution.[13,14] Rather than storing photons for a very long time, antennas are able to concentrate their energy in volumes far below the diffraction limit,[15,16] thus, achieving unparalleled emission enhancements over large bandwidths.[17]

Both microcavities and antennas also suffer from important drawbacks. Microcavities are limited in their mode volume by the diffraction limit, thus requiring high quality factors to compensate. Unfortunately, high-Q cavities are often extremely sensitive to minor fabrication errors and changes in temperature or environment, making it difficult to scale to multiple connected devices in, for example, a quantum photonic network.[5,6] Moreover, such narrow resonances typically do not match with the broad emission spectra of room temperature single-photon emitters. Antennas, on the other hand, suffer from strong radiative and dissipative losses, which limit Q to ∼10−50. This limits their application in quantum information processing, which requires emitter-antenna strong coupling, that is, coupling rates higher than the antenna loss rate.[18,19] Also, their nondirectional emission patterns tend to make efficient collection of the emission difficult. Ideally, one would be free to choose any desired Q, independent of the

Received: June 30, 2016
Published: August 29, 2016

DOI: 10.1021/acsphotonics.6b00453
ACS Photonics 2016, 3, 1943−1951

Purcell factor. An attractive candidate for such tunability is a hybrid cavity−antenna system. Recently, such systems were proposed for a selection of applications including emission enhancement,[20,21] molecule or nanoparticle detection,[22−26] nanoscale lasers,[27,28] and strong concentration near an antenna of light from free space or a waveguide.[29−32] Also, 2D Fabry-Pèrot etalons coupled to antennas have been used to study antenna-cavity coupling mechanisms.[33−35] Recent theoretical work has suggested that an emitter coupled to a high-Q cavity could gain in emission enhancement through the inclusion of a small nanoparticle.[36] Another study, however, found a strong suppression of emission enhancement for a larger, strongly scattering antenna coupled to a cavity.[37]

Here we propose hybrid systems as a versatile platform for emission enhancements that are not only significantly larger than those of cavities and antennas, but can also be tuned to work over any desired intermediate bandwidth. Using a simple but self-consistent coupled harmonic oscillator model, we show that enhancements in these systems result from a trade-off between additional losses and confinement, and we elucidate under what conditions one can profit maximally from these effects. We demonstrate for the first time that hybrid systems allow to tune the bandwidth of emission, often up to several orders of magnitude increase, while maintaining comparable or even higher emission enhancement than the bare cavity. Since our model is applicable to any cavity or antenna geometry, this provides a general guideline for designing devices that can match any desired emitter spectrum. Moreover, we propose a realistic design for a hybrid system that can be fabricated lithographically and find excellent agreement between Purcell enhancements from our model and from finite-element simulations on this design. Finally, we demonstrate that hybrid systems can boost emission enhancements while retaining a high power outcoupling efficiency into a single cavity decay channel (e.g., a waveguide), making them excellent candidates for single photon sources.

MODELING HYBRID EMISSION ENHANCEMENTS

The emission enhancement experienced by a quantum emitter due to its environment can be found by modeling the emitter as a classical oscillating dipole with constant current amplitude. The power emitted by such a drive dipole is equal to the work done by its own field on itself, that is

$$P_{\mathrm{dr}} = \frac{\omega}{2}\mathrm{Im}\{p_{\mathrm{dr}}^{*}E_{\mathrm{tot}}\} \tag{2}$$

where p_{dr} is its dipole moment, ω is its angular oscillation frequency, and E_{tot} is the total field at its position (Note that all quantities are scalars, as we have projected the fields on the axis of the antenna dipole moment and assumed the drive dipole orientation to be aligned with this axis). Dividing P_{dr} by the power that the drive dipole emits in a homogeneous medium, as given by Larmor's formula, yields the emission enhancement η, also known as the "local density of optical states" (LDOS) relative to the medium.[38] In the context of cavities, η evaluated at the cavity resonance is the Purcell factor.

Here we consider an emitter coupled to a cavity−antenna system. A possible configuration is depicted in Figure 1. However, no assumptions on either cavity or antenna geometry are made, other than that the antenna is dipolar. To obtain E_{tot}, we model cavity and antenna as harmonic oscillators and set up their coupled equations of motion (EOM).[39] We obtain (see Supporting Information)

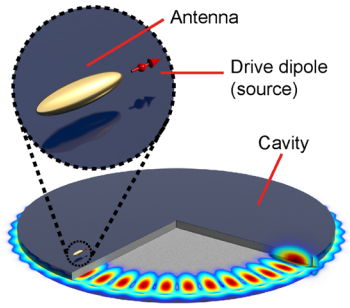

Figure 1. Coupled cavity−antenna system, driven by a dipolar source. The cavity is represented by a disk supporting a high quality factor whispering gallery mode (WGM) shown in the cut-out.

$$(\omega_0^2 - \omega^2 - i\omega\gamma)p - \beta E_{\mathrm{c}} = \beta E_{\mathrm{p,drive}} \tag{3}$$

$$-\frac{\omega^2}{\epsilon_0\epsilon V_{\mathrm{eff}}}p + (\omega_{\mathrm{c}}^2 - \omega^2 - i\omega\kappa)E_{\mathrm{c}} = \omega^2 E_{\mathrm{c,drive}} \tag{4}$$

where the free variables p and E_{c} are the antenna induced dipole moment and cavity mode field amplitude at the position of the antenna, respectively. It is easy to see that eq 3 exactly maps on a point dipole model for a polarizable plasmon antenna, driven by an external driving field $E_{\mathrm{p,drive}}$ and the cavity field.[40] Likewise, in eq 4 one recognizes the typical description of the response of a single cavity mode, driven by an external field $E_{\mathrm{c,drive}}$ and the antenna. Antenna and cavity resonance frequencies are denoted by ω_0 and ω_c, respectively, and their respective damping rates by γ and κ. Importantly, γ contains an intrinsic damping rate γ_{i} due to ohmic damping, and a frequency-dependent radiative damping rate γ_{r}, through

$$\gamma(\omega) = \gamma_{\mathrm{i}} + \gamma_{\mathrm{r}}(\omega) \tag{5}$$

Inclusion of γ_{r}, which represents antenna radiation into all modes except the cavity mode under consideration, ensures that our model is valid for both strongly and weakly scattering particles. Expressed in scattering terms, with radiation damping eq 3 represents the t-matrix of a scatterer with a consistent optical theorem for scattering, absorption, and extinction.[41] The antenna-cavity coupling is determined by the antenna oscillator strength β and the bare cavity effective mode volume V_{eff}. While in a Drude model for a metal sphere of volume V_{ant} in vacuum, β simply reads $3V_{\mathrm{ant}}\epsilon_0\omega_0^2$, in general, it may be found for any antenna by polarizability tensor retrieval from a full wave simulation.[42−44] The effective mode volume V_{eff} of the cavity equals the conventional mode volume V in eq 1 if the antenna is placed exactly at the cavity mode maximum. Away from the mode maximum, V_{eff} increases, in inverse proportion to the mode profile (see Supporting Information for an exact definition).

We may now identify $E_{\mathrm{p,drive}}$ and $E_{\mathrm{c,drive}}$ with the field generated by the drive dipole as $E_{\mathrm{p,drive}} = G_{\mathrm{bg}}\, p_{\mathrm{dr}}$ and $E_{\mathrm{c,drive}} = p_{\mathrm{dr}}/(\epsilon_0\epsilon V_{\mathrm{eff}})$, with p_{dr} the fixed dipole moment of the source. The Green's function of the background environment $G_{\mathrm{bg}} = \hat{p}\cdot\vec{G}_{\mathrm{bg}}(\mathbf{r}_{\mathrm{dr}}, \mathbf{r}_0, \omega)\cdot\hat{p}_{\mathrm{dr}}$ describes the field caused by the source at the antenna position $\mathbf{r}_0$. The same effective mode volume V_{eff} as in eq 4 appears here if we assume the cavity field at the drive dipole and antenna to be equal. This is true if the distance between them is much smaller than the wavelength. If this is not the case, our formalism remains applicable; however, one should include a complex factor in $E_{\mathrm{c,drive}}$.

DOI: 10.1021/acsphotonics.6b00453
ACS Photonics 2016, 3, 1943−1951

If we consider first the uncoupled EOMs, we can recognize the bare antenna polarizability α_{hom} and bare cavity response χ_{hom}, defined through $p = \alpha_{hom}E_{p,drive}$ and $E_c = \chi_{hom}p_{dr}$, respectively. These are $\alpha_{hom} = \beta/(\omega_0^2 - \omega^2 - i\omega\gamma)$ and $\chi_{hom} = (\omega^2/\epsilon_0\epsilon V_{eff})/(\omega_c^2 - \omega^2 - i\omega\kappa)$. When cavity and antenna are coupled, their own scattered fields act as additional driving terms, leading to the hybridized antenna polarizability α_H and cavity response function χ_H, given as (see Supporting Information)

$$\alpha_H = \alpha_{hom}(1 - \alpha_{hom}\chi_{hom})^{-1} \quad (6)$$

$$\chi_H = \chi_{hom}(1 - \alpha_{hom}\chi_{hom})^{-1} \quad (7)$$

These expressions can be viewed as response functions dressed by an infinite series of cavity−antenna interactions, similar to a multiple-scattering series in a coupled point-scatterer model.[40,45] The hybridized polarizability α_H resembles the broad, Lorentzian line shape of α_{hom}, yet with a sharp Fano-type resonance close to ω_c, similar to the polarizability discussed by Frimmer et al.[37] Increased radiation damping experienced by the antenna due to the cavity mode, as measured by Buchler et al. for a dipole near a mirror,[46] is also captured in α_H. The hybridized cavity response χ_H, on the other hand, shows a Lorentzian line shape with a resonance that is shifted and broadened exactly as predicted by the familiar Bethe-Schwinger cavity perturbation theory.[47−49]

We can now find the total field at the drive dipole position as the sum of the cavity field, the antenna scattering and the contribution of the background medium, that is, $E_{tot} = E_c + G_{bg}p + G_{bg}(\mathbf{r}_{dr}, \mathbf{r}_{dr}, \omega)p_{dr}$, where E_c and p are solved from the EOMs. Using E_{tot} in eq 2 and dividing by Larmor's formula, we obtain the emission enhancement (see Supporting Information)

$$\eta_{tot} = 1 + \frac{6\pi\epsilon_0 c^3}{\omega^3 n}\mathrm{Im}\{\alpha_H G_{bg}^2 + 2G_{bg}\alpha_H\chi_{hom} + \chi_H\} \quad (8)$$

Note that each of the terms in η_{tot} corresponds to a multiple scattering path that radiation can take, departing from and returning to the source, which will be discussed later.

ENHANCEMENT IN HYBRIDS AND BARE COMPONENTS

Using eq 8, we may now compare hybrid enhancements with those in the bare cavity and antenna. For concreteness we focus on a particular example cavity and antenna, for which Figure 2a shows enhancement spectra. Expressions for bare component enhancements can be easily derived from eq 8. For the antenna, we take $\beta = 0.12\ C^2/kg$, corresponding to a 50 nm radius sphere in vacuum with resonance frequency $\omega_0/(2\pi) = 460$ THz, and the ohmic damping rate $\gamma_i/(2\pi) = 19.9$ THz of gold.[50] We place the source at 60 nm distance from the antenna center, chosen such that we can safely neglect quenching by dark multipoles.[51] Its dipole moment points away from the antenna. This yields an emission enhancement of ∼200 at resonance. For the cavity, we assume $Q \equiv \omega_c/\kappa = 10^4$ and V_{eff} to be 10 cubic wavelengths (λ), leading to a cavity Purcell factor of 76, and typical of modest-confinement cavities, like microdisks. We present results for several different cavity resonance frequencies ω_c.

Figure 2b shows enhancement spectra for hybrid systems at various detunings. Each spectrum has two features corresponding to the two eigenmodes of the system: a broad and a narrow resonance due to modes similar to the bare antenna and the bare cavity resonance, respectively (see Supporting Information). In the remainder of this paper, we will focus only on the narrow resonance. Because the source excites both hybrid eigenmodes, the narrow resonance presents a distinct Fano-type line shape. Importantly, these Fano-resonances show peak enhancements that can far exceed those of the bare components. The hybrid system outperforms the antenna at resonance by more than a factor 3 and the cavity by more than a factor 8. At the same detuned frequency, the antenna can be outperformed by up to a factor 25 for the lowest frequency peaks shown. Similar behavior was also predicted in earlier work for much smaller, quasistatic antennas.[36] Contrary to intuition, however, the strongest enhancements are not found for a cavity and an antenna tuned to resonance, but rather for cavities significantly red-detuned from the antenna. On resonance the cavity and antenna modes destructively interfere to yield a strongly suppressed enhancement, consistent with the

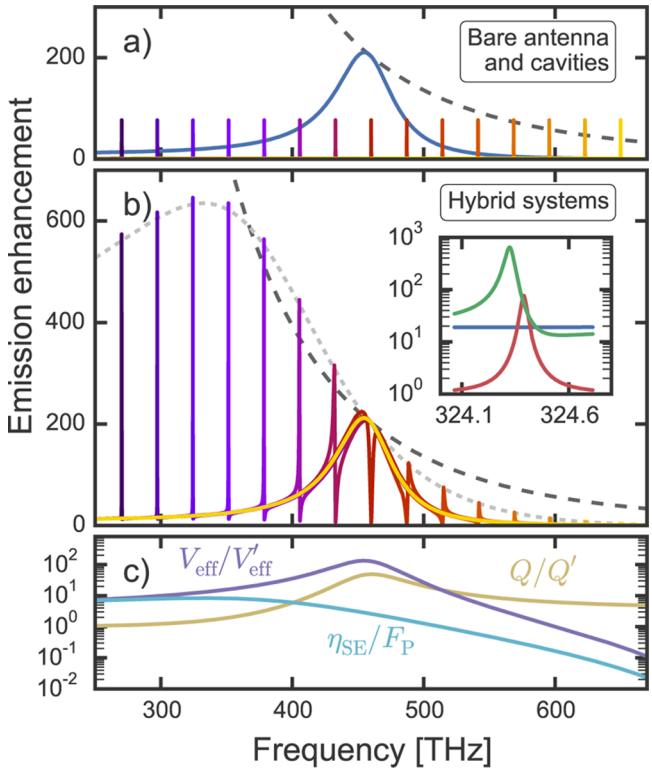

Figure 2. (a) Emission enhancement for a dipole coupled to a bare antenna (blue line) or to a set of bare cavity modes (other colors). Cavity resonances are spaced half an antenna linewidth (i.e., 27.1 THz) from each other. Each cavity peak represents a different calculation, indicated by a different color. The antenna limit η_{ant}^{lim} is shown by the dashed dark gray line. (b) Emission enhancement for the hybrid system (colored lines) composed of the same elements as shown in (a), compared to η_{ant}^{lim} (dashed dark gray line). The peak enhancement η_{SE} derived from a superemitter approximation (light gray dashed line) shows good agreement with the narrow peaks away from the antenna resonance. The inset contains a zoom-in on the peak with highest emission enhancement, showing antenna (blue), cavity (red) and hybrid (green) enhancements. (c) Broadening (yellow) and confinement (purple) of the hybrid system, approximated as a superemitter, relative to the bare cavity. The cyan line shows the ratio of the confinement and the broadening, which equals the peak enhancement of the superemitter η_{SE} relative to the bare cavity Purcell factor F_P.

DOI: 10.1021/acsphotonics.6b00453
ACS Photonics 2016, 3, 1943−1951

findings of Frimmer et al. for hybrid system with a strongly radiatively damped antenna.[37]

To understand the strong increase of emission enhancement, we can employ a "superemitter" point of view. This concept was originally proposed by Farahani et al., who claimed that an emitter coupled to an antenna could be considered as one large effective dipole when interacting with its environment.[52] In this view, for a superemitter coupled to a cavity the emitted power should be given by

$$P_{\mathrm{dr,SE}} = \frac{\omega}{2}\left|p_{\mathrm{SE}}\right|^2 \mathrm{Im}\{\chi\} \tag{9}$$

where $p_{\mathrm{SE}} = p_{\mathrm{dr}} + p = p_{\mathrm{dr}}(1 + G_{\mathrm{bg}}\alpha)$ is the effective dipole moment of the superemitter, χ is the cavity response, and α is the antenna polarizability. First intuition suggests to use both the bare polarizability α_{hom} and the bare cavity response χ_{hom}. However, Frimmer et al. demonstrated that this procedure fails to describe the dispersive Fano lineshapes and the strongly suppressed enhancement at the antenna resonance,[37] which indicates that either antenna or cavity, or both, are spoiled when tuned on resonance. Better results are obtained if the hybridized polarizability α_{H} paired with χ_{hom} is used instead. A third, alternative approach would be to use α_{hom} and the hybridized cavity response χ_{H}. Note that, compared to the full, self-consistent expression eq 8 for emission enhancements, all three superemitter descriptions are oversimplified. The merit of using α_{hom} and χ_{H} is that it accurately predicts the envelope function (gray dashed curve in Figure 2b) encompassing the Fano features. In this approach, at a hybrid resonance the emission enhancement experienced by a drive dipole in a superemitter reads $\eta_{\mathrm{SE}} = 3/(4\pi^2)Q'/V'_{\mathrm{eff}}$, with $V'_{\mathrm{eff}} = V_{\mathrm{eff}}/|1 + G_{\mathrm{bg}}\alpha_{\mathrm{hom}}|^2$ a perturbed cavity mode volume (in cubic wavelengths) and $Q' \approx \omega_c/\kappa'$, where $\kappa' = \kappa + (\omega_c/\epsilon_0\epsilon V_{\mathrm{eff}}) \times \mathrm{Im}\{\alpha_{\mathrm{hom}}(\omega_c)\}$. In the second term of κ', one recognizes the familiar result from perturbation theory, which states that a cavity resonance is broadened by the scatterer.[48] This superemitter description thus allows us to describe the emission enhancement as a balance between enhanced broadening and improved confinement.

Figure 2c shows the extra confinement $V_{\mathrm{eff}}/V'_{\mathrm{eff}}$ and broadening Q/Q' of the superemitter relative to the bare cavity. We see broadening is dominant on the blue side of the resonance because of increased radiation damping of the antenna for higher frequencies.[38] Confinement, instead, favors detunings to the red of the antenna resonance. This is due first to the lower radiation damping, and second to the positive sign of $\mathrm{Re}\{\alpha_{\mathrm{hom}}\}$, which leads to constructive interference between source and antenna when radiating into the cavity (Note that at this small antenna-source distance, G_{bg} is almost entirely real over the spectrum shown in Figure 2.) On the blue side the effect is opposite. Combined, these effects cause the emission enhancement relative to the bare cavity (cyan line in Figure 2c) to be largest on the red side of the antenna resonance. Based on the expressions for Q' and V'_{eff}, we speculate that confinement can be further boosted without increasing broadening using an antenna with stronger coupling to emitters. For instance, bow-tie antennas have similar dipole moments yet larger field enhancements (captured in G_{bg}).[53] In fact, simulations on a hybrid system composed of a nanobeam cavity and a bow-tie antenna showed a reduction of the cavity mode volume, due to inclusion of the antenna, of more than a factor 1000, with only a minor effect on Q.[26] These results show that hybrid systems can achieve the best of two worlds: a high Q-factor typical for dielectric cavities, combined with a strongly decreased mode volume due to the high field confinement by the antenna. As an example, the inset in Figure 2b shows a hybrid mode with $Q = 6.9 \times 10^3$ very similar to the bare cavity (10^4), but mode volume decreased by an order of magnitude (from $10\lambda^3$ to $0.82\lambda^3$).

BREAKING THE ANTENNA LIMIT WITH HYBRID SYSTEMS

Hybrid systems can boost not only the bare cavity enhancement, but also that of the antenna. Here we will discuss how these systems can break the fundamental limit governing antenna enhancement. This is best explained by analyzing eq 8, which indicates that three different multiple-scattering pathways contribute to the emission enhancement. We will refer to the first, second, and last terms in brackets in eq 8 as the "antenna" term, "cross-term", and "cavity" term, respectively. Figure 3 shows the hybrid enhancements from Figure 2b broken down into these three terms. Figure 3a is evidence that the antenna term, corresponding to scattering paths that start and end with an antenna−source interaction, is dominant over most of the spectrum. However, we also recognize that this term alone cannot break the bare antenna limit, shown as the gray dotted line. This limit follows from the well-known upper bound of $(3/(2\pi^2))\lambda^2$ set by energy conservation on the extinction cross section of a single dipolar scatterer.[37,54,55] Consequently, its polarizability is limited to $|\alpha^{\mathrm{lim}}| = \mathrm{Im}\{\alpha^{\mathrm{lim}}\} = (3\epsilon_0\epsilon/(4\pi^3))\lambda^3$. An antenna with an albedo $A = \gamma_r/(\gamma_i + \gamma_r)$ of 1 reaches this limit at its resonance frequency. The limit on α leads to a limit on antenna enhancement given by $\eta^{\mathrm{lim}}_{\mathrm{ant}} = 1 + (6\pi\epsilon_0 c^3/$

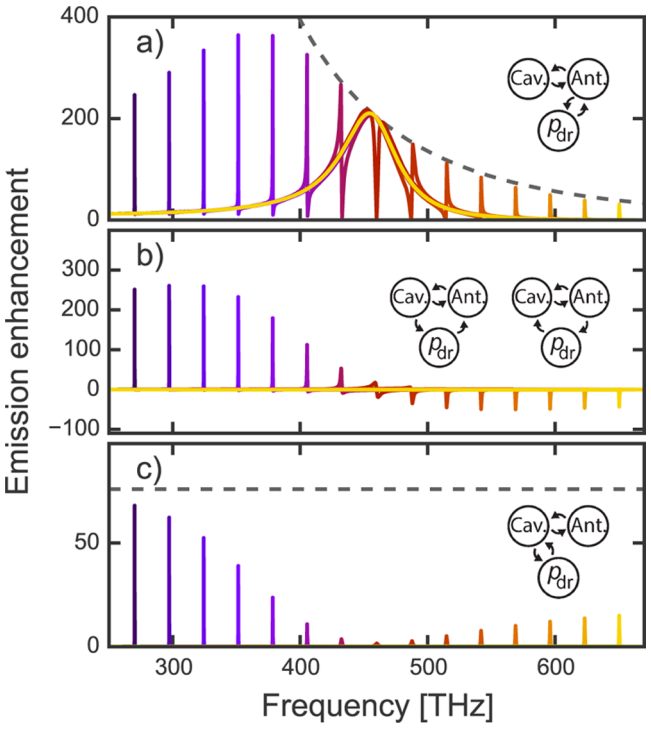

Figure 3. Emission enhancement for the hybrid system, broken down into three contributions corresponding to the terms in brackets in eq 8: the "antenna" term (a), the "cross-terms" (b), and the "cavity" term (c). Each contribution corresponds to a radiation path, which are shown in the insets. The gray dotted lines in (a) and (c) show $\eta^{\mathrm{lim}}_{\mathrm{ant}}$ and the bare cavity Purcell factor F_{P}, respectively.

DOI: 10.1021/acsphotonics.6b00453
ACS Photonics 2016, 3, 1943−1951

$(\omega^3 n))\mathrm{Im}\{\alpha^{\mathrm{lim}} G_{\mathrm{bg}}^2\} A(\omega)$. Not only a bare antenna, but also the antenna term in Figure 3a obeys this limit.

In principle there is no reason for a hybrid system, which involves a cavity mode that is not assumed to be dipolar, to be bound by the limit governing a single dipolar antenna. Yet it is tempting to think that, since the antenna has a much larger dipole moment than the source and consequently couples more strongly to the cavity, energy transfer between the source and the cavity is completely dominated by the path that passes through the antenna first. In that case, only the antenna term in Figure 3a would contribute, and the limit would be obeyed. This is because the antenna is still a dipolar scatterer bound by energy conservation, and as long as all energy passes through the antenna, enhancement is therefore also bound to the same limit. However, we see in Figure 3b,c that the cavity term and the cross-terms, all of which require direct interaction between cavity and source, contribute significantly to the enhancement. The cavity term in Figure 3c, which represents all scattering paths starting and ending with a direct source−cavity interaction, remains below the cavity Purcell factor F_{P}, since the perturbed cavity response χ_{H} is always weaker than that of the unperturbed cavity (χ_{hom}). This stands to reason, given that the antenna spoils the cavity Q. The cross-terms in Figure 3b, on the other hand, contribute strongly to the hybrid enhancement. These terms describe scattering paths starting at the antenna and ending at the cavity and vice versa. Their contribution is largest on the red side of the antenna resonance ω_0 (up to nearly half the total enhancement for the lowest frequency peaks) and switches in sign at ω_0. The sign of the cross-term indicates constructive or destructive (negative contribution) interference. In this hybrid system, the interference is between source and antenna radiation into the cavity. From Figure 2b we conclude that the sum of all three enhancement terms breaks the antenna limit, indicated by the dark dashed gray curve, for frequencies where this constructive interference takes place. Thus, through a subtle interference phenomenon, hybrids can attain larger emission enhancements than the antenna alone could ever achieve.

RANGE OF EFFECTIVE HYBRID Q AND V

Hybrid systems do not only offer increased emission enhancement, they also open up an entirely new range of quality factors and mode volumes. Figure 4 shows a "phase diagram" of Q and V. Plasmonic antennas are found in the bottom left of this diagram, at low Q and V. Conversely, cavities are in the top right, with high Q and V. However, for most applications, neither of these extrema is optimal. For example, if one desires a high Purcell factor, yet wants to avoid strong coupling, demands that are critical to a good, low-jitter single photon source,[3] the high quality factors of cavities are unpractical. A device with an intermediate Q would be ideal, provided that the Purcell factor remains high. Such an intermediate Q would also better match the emission spectrum of an emitter, which is often broader than that of a high-Q cavity yet narrower than that of an antenna.[56] Moreover, to obtain an optimal trade-off between stability and tunability, one should be able to reach this regime of intermediate Q: high Q renders cavities easily detuned by undesired perturbations, whereas the very low Q of antennas makes them difficult to tune. Here we will show that hybrid systems allow precisely this: choosing the Q-factor to a desired, intermediate value, while retaining or even improving on the bare cavity Purcell factor.

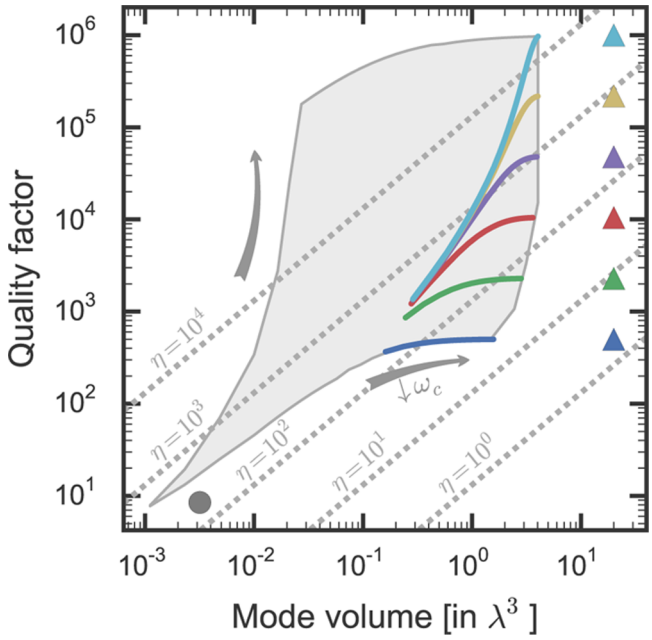

Figure 4. Phase diagram of quality factors Q and dimensionless mode volumes V/λ^3. Shown are the values for the bare antenna (dark circle) and a set of bare cavities (▲), as well as the values of the corresponding hybrid modes. The colored lines show hybrid results for all cavity−antenna detunings used. For decreasing ω_c, that is, further red-detuning of the cavity, hybrid Q and V lie closer to those of the bare cavity. The light gray area indicates the location of the hybrid values attained for cavities with $500 < Q < 10^6$ and $0.5^3 < V_{\mathrm{eff}}/\lambda^3 < 20$. Dashed gray lines are lines of constant emission enhancement η.

In Figure 4, we compare Q and V_{eff} of modes in hybrid systems with those in the bare cavities and antenna. We assume the same antenna as in Figures 2 and 3. Cavities were used with $500 < Q < 10^6$ and $0.5^3 < V_{\mathrm{eff}}/\lambda^3 < 20$, and for each combination of Q and $V_{\mathrm{eff}}/\lambda^3$ we take several cavity resonance frequencies 100 THz $< \omega_c <$ 433 THz, corresponding to cavity−antenna detunings ranging from 0.5 to 6.6 antenna linewidths. Cavities were always red-detuned from the antenna. To position hybrid structures in this diagram, we calculate emission enhancement for frequencies around the cavity resonance. We retrieve Q from the linewidth of the Fano-resonance (see Supporting Information). While mode volume is only well-defined for a single (nonleaky) mode,[57−60] here we employ an operational definition through Purcell's formula (eq 1) and the peak value of the emission enhancement ($\eta_{\mathrm{tot}}^{\mathrm{peak}}$). This leads to $V_{\mathrm{eff}}^{\mathrm{hyb}} = (3/(4\pi^2))Q/\eta_{\mathrm{tot}}^{\mathrm{peak}}$, with $V_{\mathrm{eff}}^{\mathrm{hyb}}$ in units of the cubic resonance wavelength. We use the same definition for the antenna mode volume. Note that, because we keep cavity Q and $V_{\mathrm{eff}}/\lambda^3$ constant when varying ω_c, cavities with different ω_c appear at the same point in Figure 4. Hybrid Q and V, however, depend strongly on cavity−antenna detuning, as we have seen in Figure 2. Therefore, the hybrid systems composed of cavities with different ω_c appear as lines in Figure 4.

From Figure 4 we see that hybrid systems provide exactly the tunability discussed earlier: through variation of the cavity−antenna detuning, any practical Q between that of the cavity and the antenna can be chosen. The subset displayed in color shows that this extreme tunability typically does not come at the price of Purcell enhancement. If the bare cavity provides an enhancement far below that of the antenna (blue and green), hybrid systems can gain strongly in Purcell enhancement

DOI: 10.1021/acsphotonics.6b00453
ACS Photonics 2016, 3, 1943−1951

compared to the cavity, yet the Q-factor remains close to that of the bare cavity. For cavities with enhancements similar to the bare antenna (red, purple and yellow), one can gain with respect to both bare components, and Q can be tuned over a large range while maintaining very high enhancement. As can be expected, the Purcell factor of the cavities with highest Q (light blue) is reduced by inclusion of the antenna, as cavities with such narrow resonances are easily spoiled by the losses introduced by an antenna. Yet it is remarkable that enhancements of order 10^3 can be maintained over a large range of strongly reduced Q-factors in such systems. To illustrate the full attainable range of hybrid Q and V, the light gray area shows where all the hybrid systems are located, for the full range of cavities examined here. From this we see that any Q between that of the cavity and the antenna can be obtained, at high Purcell factor. In summary, hybrid systems can bridge the gap in Q and V_{eff} between cavities and plasmonic antennas, reaching any desired, practical Q at similar or better enhancement factors.

FINITE-ELEMENT SIMULATIONS ON A REALISTIC HYBRID SYSTEM

Here we analyze a possible physical implementation of the proposed hybrid systems. We perform finite-element simulations on a realistic cavity−antenna design using COMSOL Multiphysics 5.1, which also serve to verify the validity of our analytical oscillator model. Figure 1 is an artistic representation of the simulations. As a cavity, we take a silicon nitride (n = 1.997) disk in vacuum with a radius of 2032 nm and a thickness of 200 nm. To tune the cavity Q and to help trace how much power flows into the cavity mode we include a small amount of absorption as imaginary component (4×10^{-6}) in the permittivity of the silicon nitride. The disk supports a radially polarized m = 22 whispering gallery mode (WGM) at 382.584 THz (~784 nm) with $Q = 7.28 \times 10^4$ (see Figure 5a,c). The antenna we use is a gold prolate ellipsoid with a long (short) axis radius of 70 (20) nm. Optical constants are described by a modified Drude model.[50] Figure 5b shows the antenna field profile. The hybrid systems is obtained by placing the antenna 50 nm above the disk, just next to the source. In an experiment, one could use an antenna that is fabricated (e.g., by e-beam lithography) directly on top of the disk, as demonstrated earlier for similar geometries.[27,61]

To verify the predictions of the oscillator model, we first calculate emission enhancement spectra for the bare components, and through a fit retrieve all the input parameters for our oscillator model. We then compare the oscillator model prediction for the enhancement spectrum of the hybrid to that obtained from finite-element simulation of the hybrid system.

From the fit to the bare cavity emission and absorption spectra (see Supporting Information), we find the cavity parameters ω_c, $\kappa_r/2\pi$ = 5 GHz, $\kappa_{abs}/2\pi$ = 0.3 GHz, and V_{eff} = $22.8\lambda^3$. This leads to a peak enhancement of 242. The bare antenna spectra yield the antenna parameters $\omega_0/2\pi$ = 436 THz, $\gamma_i/2\pi$ = 18.1 THz, β = 0.073 C^2/kg, and an effective source−antenna distance of 55.2 nm (smaller than the physical source-to-center distance of 70 + 12 nm owing to the lightning rod effect). These values lead to a bare radiative (absorptive) antenna emission enhancement of 186 (174) at maximum. Figure 6 shows the comparison between the oscillator model prediction based on these values and the full simulations on the hybrid system where the antenna was placed beside the source, just above the disk, as shown in Figure 5d. We find an emission

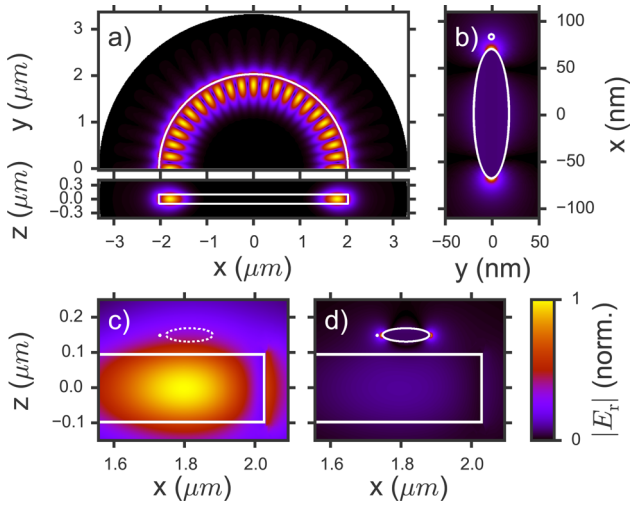

Figure 5. Cross-cuts of the cavity, antenna and hybrid mode profiles. All fields are normalized to their maximum values. Cross-cuts are taken at symmetry planes of the structures. White lines indicate the edges of the structures. (a) Top view and side view of the bare cavity eigenmode. Only the dominant (radial) field component is shown. (b) Field profile of the bare antenna in vacuum, illuminated by an x-polarized plane wave at its resonance frequency. The x-component of the scattered field is shown. The small white circle above the antenna tip indicates where we will place the source dipole. (c) Zoom-in of the bare cavity eigenmode profile. The position of the antenna in the hybrid system is indicated with the dashed line. Note that no antenna was used in this simulation. The position of the drive dipole is indicated beside the antenna tip. (d) Zoom-in of the hybrid eigenmode profile. Hot spots are visible near the antenna tips.

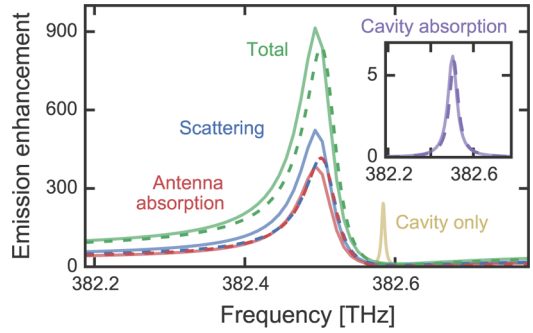

Figure 6. Emission enhancements in a hybrid system from the oscillator model (dashed) and from simulations (solid). We show enhancements due to scattering into free space (blue), antenna absorption (red) and total enhancement (green). Enhancement due to cavity absorption (purple) in the hybrid system is visible in the inset. Enhancement from the bare cavity (yellow) is shown for comparison.

enhancement of ~914 in the hybrid system, which is a large increase with respect to the bare cavity (242) and antenna (360 at resonance and ~65 near cavity resonance). The bandwidth over which this enhancement occurs is increased by a factor 9.4 (to 49 GHz) with respect to the cavity. There is excellent agreement between the model and the simulation for all components of the enhancement. Remaining differences can be largely attributed to errors in the antenna fit (see Supporting Information). These results demonstrate that the oscillator model correctly predicts emission enhancement in a coupled cavity−antenna system, based on the response of the bare components. Moreover, it shows that a realistic cavity−antenna system can combine the best features of both cavity and

DOI: 10.1021/acsphotonics.6b00453
ACS Photonics 2016, 3, 1943−1951

antenna, achieving much stronger emission enhancement than the bare components.

EFFICIENCY OF RADIATION INTO THE CAVITY

In the previous sections, we demonstrated that hybrid systems allow strongly boosted emission enhancements at any desired quality factor Q. Here we will show that one can also control by hybridization into what channels energy is emitted. Depending on the application, one may, for example, wish to design a system that emits all power into free-space or, rather, into a single-mode waveguide. The latter is often the case for an on-chip single-photon source, for example. From the equations of motions, we can also deduce the power dissipated in the antenna, the power radiated by the antenna into free space,[62] and the power emitted into the cavity decay channel (see Supporting Information). Here we use this to study the fraction of power going into the cavity decay channel, as this is usually most efficiently extracted in, for example, a waveguide. This fraction, that is, the efficiency of extraction into single mode output channel, is also known as the β-factor in the context of single-photon sources.[3] Note that, as we generally have not specified the origin of the cavity loss κ, one could assume it to be dominated by outcoupling to a waveguide. In experiments this is commonly achieved by evanescent coupling of a cavity to a nearby integrated waveguide or fiber taper.[63,64] Overcoupling then ensures that the waveguide or taper is the dominant loss channel.

Figure 7a,b shows the relative cavity outflux and the peak value of the total hybrid emission enhancement η_{tot}^{peak} as a function of cavity resonance ω_c and bare cavity Purcell factor F_P. The same cavities and antenna were used as in Figure 4, and detuning now ranged between 0 and 6.6 antenna linewidths. Note that relative cavity outflux and η_{tot}^{peak} are fully determined by antenna properties, detuning and F_P (i.e., Q/V_{eff}), not by Q and V_{eff} separately. There is a large region in which hybrid emission enhancement can be increased with respect to the cavity, while maintaining a very high fraction of power flux into the cavity channel. This implies that the plasmonic antenna helps to boost emission enhancement through its field confinement while adding almost no additional losses, consistent with the results in Figure 2c. Figure 7 shows that this works particularly well for cavities with F_P between 10 and $\sim 10^3$. Close to the antenna resonance (460 THz), cavity outflux drops as power outflux is dominated by the antenna. For very good cavities with F_P around 10^4, power outflux is also dominated by the antenna, even for far red-detunings. This reflects the fact that either intrinsic cavity losses are very low (high Q) or coupling to the antenna is very strong (low V). Both cases lead to the antenna decay channels being dominant. Importantly, dominant outcoupling through the antenna does not mean that all the power is dissipated: it is distributed between dipolar radiation and dissipation according to the bare antenna albedo. For applications where radiative efficiency rather than coupling to a waveguide is important, these antenna-dominated regimes can be highly interesting.

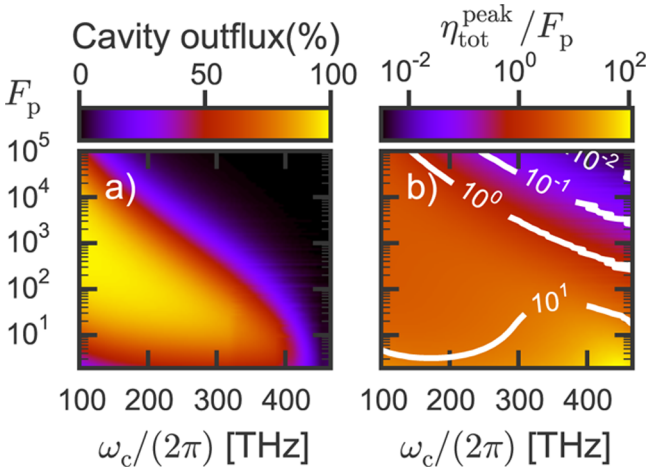

Figure 7. (a) Fraction of power into the cavity decay channel κ, as a function of cavity resonance ω_c and bare cavity Purcell factor F_P. This fraction was evaluated at the peak of the total emission enhancement η_{tot}. We use the same antenna as in Figures 2 and 4. (b) Total emission enhancement η_{tot}^{peak} of the hybrid system (at peak) relative to F_P. The same cavities and antenna were used as in (a).

In conclusion, one can generally engineer the system in such a way that the power flows in any of the desired channels. Specifically, we have shown that it can be designed for a high extraction efficiency into a single cavity loss channel, such as a waveguide. This is of particular interest for applications such as an on-chip single-photon source with a high β-factor.

CONCLUSIONS AND OUTLOOK

We have shown that hybrid cavity−antenna systems can achieve larger emission enhancement than either the antenna or the cavity alone. These systems can benefit simultaneously from the high cavity quality factor and the low mode volume of the antenna. This benefit occurs only when the cavity is red-detuned from the antenna. We have demonstrated that this is partly due to the reduced radiation damping of the antenna, and partly due to constructively interfere between source and antenna radiation. The latter also allows the enhancements in hybrid systems to break the fundamental limit governing antenna enhancements. Moreover, we have shown that hybrid structures allow to design any desired quality factor while maintaining similar or higher emission enhancement than the bare cavity and antenna. A study of the cavity power outflux as a fraction of total emitted power demonstrated that one can furthermore engineer the system to emit efficiently into a desired output channel, such as a waveguide. Finally, a physical implementation using a WGM cavity and a gold antenna was proposed and tested using finite-element simulations, showing strongly increased emission enhancement and excellent agreement with the oscillator model.

These results highlight hybrid systems as a highly versatile and promising platform for enhancement of light-matter interactions. Such systems can leverage the existing expertise on high-Q cavities and plasmonic antennas for devices that combine the best of both worlds, while avoiding the disadvantages such as losses in the metal. While one has to pay the price of a multistep fabrication process to integrate cavity, antenna and emitter, the advantage is that it could open up arbitrary bandwidth cavity QED to fit a wide variety of emitters, including single molecules, quantum dot nanocrystals and nanodiamond color centers. This paves the way to further studies, such as an experimental demonstration of Purcell enhancements in the proposed design or studies of hybrid systems as efficient interfaces between free-space radiation and on-chip waveguides.

DOI: 10.1021/acsphotonics.6b00453
ACS Photonics 2016, 3, 1943−1951

■ ASSOCIATED CONTENT

Supporting Information

The Supporting Information is available free of charge on the ACS Publications website at DOI: 10.1021/acsphotonics.6b00453.

Derivation of the equations of motion and the hybrid emission enhancement (total enhancement as well as the fractions in the separate decay channels), further information about the hybridized polarizability α_H and cavity response χ_H, and details of the finite-element simulations on a hybrid system (PDF).

■ AUTHOR INFORMATION

Corresponding Authors

*E-mail: h.doeleman@amolf.nl (H.M.D.).
*E-mail: f.koenderink@amolf.nl (A.F.K.).

Notes

The authors declare no competing financial interest.

■ ACKNOWLEDGMENTS

This work is part of the research program of the Foundation for Fundamental Research on Matter (FOM), which is financially supported by The Netherlands Organization for Scientific Research (NWO). The authors gratefully acknowledge Ben van Linden van den Heuvell, Klaasjan van Druten, Robert Spreeuw, Francesco Monticone, and Andrea Alù for inspiring discussions, and Henk-Jan Boluijt for the designs used in Figure 1.

■ REFERENCES

(1) Lounis, B.; Orrit, M. Single-photon sources. *Rep. Prog. Phys.* **2005**, *68*, 1129−1179.
(2) Eisaman, M. D.; Fan, J.; Migdall, A.; Polyakov, S. V. Invited Review Article: Single-photon sources and detectors. *Rev. Sci. Instrum.* **2011**, *82*, 071101.
(3) Lodahl, P.; Mahmoodian, S.; Stobbe, S. Interfacing single photons and single quantum dots with photonic nanostructures. *Rev. Mod. Phys.* **2015**, *87*, 347−400.
(4) Hill, M. T.; Gather, M. C. Advances in small lasers. *Nat. Photonics* **2014**, *8*, 908−918.
(5) Kimble, H. J. The quantum internet. *Nature* **2008**, *453*, 1023−30.
(6) O'Brien, J. L.; Furusawa, A.; Vučković, J. Photonic quantum technologies. *Nat. Photonics* **2009**, *3*, 687−695.
(7) Anker, J. N.; Hall, W. P.; Lyandres, O.; Shah, N. C.; Zhao, J.; Van Duyne, R. P. Biosensing with plasmonic nanosensors. *Nat. Mater.* **2008**, *7*, 442−53.
(8) Qavi, A. J.; Washburn, A. L.; Byeon, J.-Y.; Bailey, R. C. Label-free technologies for quantitative multiparameter biological analysis. *Anal. Bioanal. Chem.* **2009**, *394*, 121−35.
(9) Vollmer, F.; Yang, L.; Fainman, S. Label-free detection with high-Q microcavities: A review of biosensing mechanisms for integrated devices. *Nanophotonics* **2012**, *1*, 267−291.
(10) Purcell, E. M. Spontaneous emission probabilities at radio frequencies. *Phys. Rev.* **1946**, *69*.
(11) Vahala, K. J. Optical microcavities. *Nature* **2003**, *424*, 839−846.
(12) Arcari, M.; Söllner, I.; Javadi, A.; Lindskov Hansen, S.; Mahmoodian, S.; Liu, J.; Thyrrestrup, H.; Lee, E. H.; Song, J. D.; Stobbe, S.; Lodahl, P. Near-Unity Coupling Efficiency of a Quantum Emitter to a Photonic Crystal Waveguide. *Phys. Rev. Lett.* **2014**, *113*, 093603.
(13) Novotny, L.; van Hulst, N. F. Antennas for light. *Nat. Photonics* **2011**, *5*, 83−90.
(14) Tame, M. S.; McEnery, K. R.; Özdemir, Ş. K.; Lee, J.; Maier, S. A.; Kim, M. S. Quantum plasmonics. *Nat. Phys.* **2013**, *9*, 329−340.
(15) Gramotnev, D. K.; Bozhevolnyi, S. I. Plasmonics beyond the diffraction limit. *Nat. Photonics* **2010**, *4*, 83−91.
(16) Schuller, J. A.; Barnard, E. S.; Cai, W.; Jun, Y. C.; White, J. S.; Brongersma, M. L. Plasmonics for extreme light concentration and manipulation. *Nat. Mater.* **2010**, *9*, 193−204.
(17) Akselrod, G. M.; Argyropoulos, C.; Hoang, T. B.; Ciracì, C.; Fang, C.; Huang, J.; Smith, D. R.; Mikkelsen, M. H. Probing the mechanisms of large Purcell enhancement in plasmonic nanoantennas. *Nat. Photonics* **2014**, *8*, 835−840.
(18) Kimble, H. J. Strong Interactions of Single Atoms and Photons in Cavity QED. *Phys. Scr.* **1998**, *T76*, 127.
(19) Raimond, J. M.; Brune, M.; Haroche, S. Manipulating quantum entanglement with atoms and photons in a cavity. *Rev. Mod. Phys.* **2001**, *73*, 565−582.
(20) Barth, M.; Schietinger, S.; Fischer, S.; Becker, J.; Nüsse, N.; Aichele, T.; Löchel, B.; Sönnichsen, C.; Benson, O. Nanoassembled plasmonic-photonic hybrid cavity for tailored light-matter coupling. *Nano Lett.* **2010**, *10*, 891−5.
(21) Boriskina, S. V.; Reinhard, B. M. Spectrally and spatially configurable superlenses for optoplasmonic nanocircuits. *Proc. Natl. Acad. Sci. U. S. A.* **2011**, *108*, 3147−51.
(22) De Angelis, F.; Patrini, M.; Das, G.; Maksymov, I.; Galli, M.; Businaro, L.; Andreani, L. C.; Di Fabrizio, E. A hybrid plasmonic-photonic nanodevice for label-free detection of a few molecules. *Nano Lett.* **2008**, *8*, 2321−7.
(23) Dantham, V. R.; Holler, S.; Barbre, C.; Keng, D.; Kolchenko, V.; Arnold, S. Label-Free Detection of Single Protein Using a Nanoplasmonic-Photonic Hybrid Microcavity. *Nano Lett.* **2013**, *13*, 3347−3351.
(24) Santiago-Cordoba, M. A.; Cetinkaya, M.; Boriskina, S. V.; Vollmer, F.; Demirel, M. C. Ultrasensitive detection of a protein by optical trapping in a photonic-plasmonic microcavity. *J. Biophotonics* **2012**, *5*, 629−638.
(25) Hu, Y.-W.; Li, B.-B.; Liu, Y.-X.; Xiao, Y.-F.; Gong, Q. Hybrid photonic-plasmonic mode for refractometer and nanoparticle trapping. *Opt. Commun.* **2013**, *291*, 380−385.
(26) Conteduca, D.; Dell'Olio, F.; Innone, F.; Ciminelli, C.; Armenise, M. N. Rigorous design of an ultra-high Q/V photonic/plasmonic cavity to be used in biosensing applications. *Opt. Laser Technol.* **2016**, *77*, 151−161.
(27) Zhang, T.; Callard, S.; Jamois, C.; Chevalier, C.; Feng, D.; Belarouci, A. Plasmonic-photonic crystal coupled nanolaser. *Nanotechnology* **2014**, *25*, 315201.
(28) Mivelle, M.; Viktorovitch, P.; Baida, F. I.; El Eter, A.; Xie, Z.; Vo, T.-P.; Atie, E.; Burr, G. W.; Nedeljkovic, D.; Rauch, J.-Y.; Callard, S.; Grosjean, T. Light funneling from a photonic crystal laser cavity to a nano-antenna: overcoming the diffraction limit in optical energy transfer down to the nanoscale. *Opt. Express* **2014**, *22*, 15075−87.
(29) Chamanzar, M.; Adibi, A. Hybrid nanoplasmonic-photonic resonators for efficient coupling of light to single plasmonic nanoresonators. *Opt. Express* **2011**, *19*, 22292.
(30) Ahn, W.; Boriskina, S. V.; Hong, Y.; Reinhard, B. M. Photonic-plasmonic mode coupling in on-chip integrated optoplasmonic molecules. *ACS Nano* **2012**, *6*, 951−60.
(31) Ren, F.; Takashima, H.; Tanaka, Y.; Fujiwara, H.; Sasaki, K. Two-photon excited fluorescence from a pseudoisocyanine-attached gold tip via a plasmonic-photonic hybrid system. *Opt. Express* **2015**, *23*, 21730−21740.
(32) Ahn, W.; Zhao, X.; Hong, Y.; Reinhard, B. M. Low-Power Light Guiding and Localization in Optoplasmonic Chains Obtained by Directed Self-Assembly. *Sci. Rep.* **2016**, *6*, 22621.
(33) Ameling, R.; Giessen, H. Cavity plasmonics: large normal mode splitting of electric and magnetic particle plasmons induced by a photonic microcavity. *Nano Lett.* **2010**, *10*, 4394−8.
(34) Vázquez-Guardado, A.; Safaei, A.; Modak, S.; Franklin, D.; Chanda, D. Hybrid Coupling Mechanism in a System Supporting High Order Diffraction, Plasmonic, and Cavity Resonances. *Phys. Rev. Lett.* **2014**, *113*, 263902.
(35) Bahramipanah, M.; Dutta-Gupta, S.; Abasahl, B.; Martin, O. J. F. Cavity-Coupled Plasmonic Device with Enhanced Sensitivity and Figure-of-Merit. *ACS Nano* **2015**, *9*, 7621−7633.

DOI: 10.1021/acsphotonics.6b00453
ACS Photonics 2016, 3, 1943−1951

(36) Xiao, Y.-F.; Liu, Y.-C.; Li, B.-B.; Chen, Y.-L.; Li, Y.; Gong, Q. Strongly enhanced light-matter interaction in a hybrid photonic-plasmonic resonator. *Phys. Rev. A: At., Mol., Opt. Phys.* **2012**, *85*, 031805.
(37) Frimmer, M.; Koenderink, A. F. Superemitters in hybrid photonic systems: A simple lumping rule for the local density of optical states and its breakdown at the unitary limit. *Phys. Rev. B: Condens. Matter Mater. Phys.* **2012**, *86*, 235428.
(38) Novotny, L.; Hecht, B. *Principles of Nano-Optics*; Cambridge University Press, 2012.
(39) Haroche, S. Cavity Quantum Electrodynamics. *AIP Conf. Proc.* **1992**, 45.
(40) Lagendijk, A.; van Tiggelen, B. A. Resonant multiple scattering of light. *Phys. Rep.* **1996**, *270*, 143−215.
(41) de Vries, P.; van Coevorden, D.; Lagendijk, A. Point scatterers for classical waves. *Rev. Mod. Phys.* **1998**, *70*, 447−466.
(42) Bohren, C. F.; Huffman, D. R. *Absorption and Scattering of Light by Small Particles*; Wiley, 1983.
(43) Bernal Arango, F.; Koenderink, A. F. Polarizability tensor retrieval for magnetic and plasmonic antenna design. *New J. Phys.* **2013**, *15*, 073023.
(44) Bernal Arango, F.; Coenen, T.; Koenderink, A. F. Underpinning Hybridization Intuition for Complex Nanoantennas by Magneto-electric Quadrupolar Polarizability Retrieval. *ACS Photonics* **2014**, *1*, 444−453.
(45) García de Abajo, F. J. Colloquium: Light scattering by particle and hole arrays. *Rev. Mod. Phys.* **2007**, *79*, 1267−1290.
(46) Buchler, B. C.; Kalkbrenner, T.; Hettich, C.; Sandoghdar, V. Measuring the quantum efficiency of the optical emission of single radiating dipoles using a scanning mirror. *Phys. Rev. Lett.* **2005**, *95*, 063003.
(47) Bethe, H.; Schwinger, J. *Perturbation Theory for Cavities*; Massachusetts Institute of Technology, Radiation Laboratory, 1943.
(48) Waldron, R. Perturbation theory of resonant cavities. *Proc. Inst. Electr. Eng., Part C* **1960**, *107*, 272.
(49) Ruesink, F.; Doeleman, H. M.; Hendrikx, R.; Koenderink, A. F.; Verhagen, E. Perturbing Open Cavities: Anomalous Resonance Frequency Shifts in a Hybrid Cavity-Nanoantenna System. *Phys. Rev. Lett.* **2015**, *115*, 203904.
(50) Penninkhof, J. J.; Sweatlock, L. A.; Moroz, A.; Atwater, H. A.; van Blaaderen, A.; Polman, A. Optical cavity modes in gold shell colloids. *J. Appl. Phys.* **2008**, *103*, 123105.
(51) Mertens, H.; Polman, A. Strong luminescence quantum-efficiency enhancement near prolate metal nanoparticles: Dipolar versus higher-order modes. *J. Appl. Phys.* **2009**, *105*, 044302.
(52) Farahani, J. N.; Pohl, D. W.; Eisler, H.-J.; Hecht, B. Single Quantum Dot Coupled to a Scanning Optical Antenna: A Tunable Superemitter. *Phys. Rev. Lett.* **2005**, *95*, 017402.
(53) Kinkhabwala, A.; Yu, Z.; Fan, S.; Avlasevich, Y.; Müllen, K.; Moerner, W. E. Large single-molecule fluorescence enhancements produced by a bowtie nanoantenna. *Nat. Photonics* **2009**, *3*, 654−657.
(54) Foot, C. *Atomic Physics*; Oxford University Press: Oxford, 2005; pp 140−142.
(55) Ruan, Z.; Fan, S. Design of subwavelength superscattering nanospheres. *Appl. Phys. Lett.* **2011**, *98*, 043101.
(56) Englund, D.; Fattal, D.; Waks, E.; Solomon, G.; Zhang, B.; Nakaoka, T.; Arakawa, Y.; Yamamoto, Y.; Vuković, J. Controlling the spontaneous emission rate of single quantum dots in a two-dimensional photonic crystal. *Phys. Rev. Lett.* **2005**, *95*, 013904.
(57) Koenderink, A. F. On the use of Purcell factors for plasmon antennas. *Opt. Lett.* **2010**, *35*, 4208−10.
(58) Kristensen, P. T.; Van Vlack, C.; Hughes, S. Generalized effective mode volume for leaky optical cavities. *Opt. Lett.* **2012**, *37*, 1649−51.
(59) Sauvan, C.; Hugonin, J. P.; Maksymov, I. S.; Lalanne, P. Theory of the Spontaneous Optical Emission of Nanosize Photonic and Plasmon Resonators. *Phys. Rev. Lett.* **2013**, *110*, 237401.
(60) Yang, J.; Perrin, M.; Lalanne, P. Analytical Formalism for the Interaction of Two-Level Quantum Systems with Metal Nano-resonators. *Phys. Rev. X* **2015**, *5*, 021008.
(61) Guo, R.; Rusak, E.; Staude, I.; Dominguez, J.; Decker, M.; Rockstuhl, C.; Brener, I.; Neshev, D. N.; Kivshar, Y. S. Multipolar Coupling in Hybrid Metal-Dielectric Metasurfaces. *ACS Photonics* **2016**, *3*, 349−353.
(62) Mertens, H.; Koenderink, A. F.; Polman, A. Plasmon-enhanced luminescence near noble-metal nanospheres: Comparison of exact theory and an improved Gersten and Nitzan model. *Phys. Rev. B: Condens. Matter Mater. Phys.* **2007**, *76*, 115123.
(63) Knight, J. C.; Cheung, G.; Jacques, F.; Birks, T. A. Phase-matched excitation of whispering-gallery-mode resonances by a fiber taper. *Opt. Lett.* **1997**, *22*, 1129.
(64) Spillane, S. M.; Kippenberg, T. J.; Painter, O. J.; Vahala, K. J. Ideality in a fiber-taper-coupled microresonator system for application to cavity quantum electrodynamics. *Phys. Rev. Lett.* **2003**, *91*, 043902.

DOI: 10.1021/acsphotonics.6b00453
ACS Photonics 2016, 3, 1943−1951